Human Molecular Genetics, 2015, Vol. 24, No. 22 6505–6514

doi: 10.1093/hmg/ddv359
Advance Access Publication Date: 11 September 2015
Original Article

ORIGINAL ARTICLE

Accelerated reproductive aging in females lacking a novel centromere protein SYCP2L

Jian Zhou[1,2], Paula Stein[3], N. Adrian Leu[1], Lukáš Chmátal[3], Jiangyang Xue[1,4], Jun Ma[1,3], Xiaoyan Huang[4], Michael A. Lampson[3], Richard M. Schultz[3] and P. Jeremy Wang[1,*]

[1]Department of Biomedical Sciences, University of Pennsylvania School of Veterinary Medicine, 3800 Spruce Street, Philadelphia, PA 19104, USA, [2]Xinhua Hospital, Shanghai Jiao Tong University School of Medicine, Shanghai 200092, China, [3]Department of Biology, University of Pennsylvania, 433 South University Avenue, Philadelphia, PA 19104, USA and [4]State Key Laboratory of Reproductive Medicine, Nanjing Medical University, Nanjing 210029, China

*To whom correspondence should be addressed. Tel: +1 2157460160; Fax: +1 2155736810; Email: pwang@vet.upenn.edu

Abstract

Menopause results from loss of ovarian function and marks the end of a woman's reproductive life. Alleles of the human *SYCP2L* locus are associated with age at natural menopause (ANM). SYCP2L is a paralogue of the synaptonemal complex protein SYCP2 and is expressed exclusively in oocytes. Here we report that SYCP2L localizes to centromeres of dictyate stage oocytes, which represent the limited pool of primordial oocytes that are formed perinatally and remain arrested till ovulation. Centromere localization of SYCP2L requires its C-terminal portion, which is missing in truncated variants resulting from low-frequency nonsense mutations identified in humans. Female mice lacking SYCP2L undergo a significantly higher progressive loss of oocytes with age compared with wild-type females and are less fertile. Specifically, the pool of primordial oocytes becomes more rapidly depleted in SYCP2L-deficient than in wild-type females, such that with aging, fewer oocytes undergo maturation in developing follicles. We find that a human *SYCP2L* intronic single nucleotide polymorphism (SNP) rs2153157, which is associated with ANM, changes the splicing efficiency of U12-type minor introns and may therefore regulate the steady-state amount of *SYCP2L* transcript. Furthermore, the more efficiently spliced allele of this intronic SNP in *SYCP2L* is associated with increased ANM. Our results suggest that SYCP2L promotes the survival of primordial oocytes and thus provide functional evidence for its association with ANM in humans.

Introduction

Menopause, cessation of ovarian function, marks the end of a woman's reproductive life. Ovarian aging is attributed to a continuous decline in oocyte number and quality with increasing age. Age at natural menopause (ANM) is a known risk factor for a number of chronic diseases. Early menopause (menopause before the age of 45 years) is a risk factor for increased mortality, coronary heart disease and osteoporosis (1–3). Late menopause (menopause at the age of 54 years and later) is associated with increased risk of breast cancer (4). Recent genome-wide association studies (GWAS) have identified more than 20 genetic loci that are associated with ANM (5–9). Most of these loci encode factors that appear to be involved in DNA repair and immune response (7). For some of these candidate factors, potential molecular mechanisms that mediate a specific ovarian function are emerging. For instance, MCM8 is associated with ANM by GWAS (5,8,9) and *MCM8* mutations cause premature ovarian failure in humans (10). MCM8 functions in homologous

Received: June 8, 2015. **Revised:** August 7, 2015. **Accepted:** September 1, 2015

recombination and *Mcm8*-deficient female mice are sterile due to a failure in oogenesis (11,12). However, the role of most ANM-associated factors in the regulation of ovarian function is not known.

In mammals, shortly after sex determination in the developing embryo, primordial germ cells in females enter meiosis, a cell division unique to germ cells (13–15). Oocytes progress through the early stages of the first meiotic prophase—leptotene, zygotene and pachytene—and arrest at the diplotene stage prior to birth. Oocytes remain in prophase I arrest until ovulation, during which they resume meiosis and typically arrest at metaphase II. During meiosis, homologous chromosomes undergo pairing, synapsis and recombination (16,17). Chromosomal synapsis is mediated by formation of a synaptonemal complex (SC), which is a tripartite structure consisting of two lateral/axial elements and a central element (18,19). Proteins constituting the SC have been identified in a number of species. In mouse, SYCP2 and SYCP3 are components of the lateral/axial elements (20–23). The central element consists of SYCE1, SYCE2, SYCE3 and TEX12 (24–29). Transverse filaments, comprised of SYCP1, physically link the lateral elements to the central element, resulting in chromosomal synapsis (30–32). Genetic studies demonstrate that the SC is essential for chromosomal synapsis and meiotic recombination in mammals (22,23,25–27,31).

SYCP2L (SYCP2-like) is an uncharacterized sequence homologue of SYCP2. Recent GWAS studies have shown that variants of the human *SYCP2L* locus were associated with ANM (5,8). SYCP2L is conserved in vertebrates from *Xenopus* to humans (33). In *Xenopus* oocytes, SYCP2L (also known as NO145) is a major constituent of the nucleolar cortical skeleton (33). *Xenopus* SYCP2L protein is exclusively expressed in immature oocytes before germinal vesicle (GV) breakdown (i.e. nuclear membrane breakdown) and is rapidly degraded by proteasomes during meiotic maturation (33). SYCP2L is nuclear in human oocytes and localizes as dot-like structures in bovine oocytes (33). Despite these cell biological studies, the function of SYCP2L in oocytes remains unknown. Here, we report that SYCP2L is a novel centromere protein in oocytes and demonstrate that SYCP2L promotes the survival of reserve oocytes and regulates reproductive aging in females.

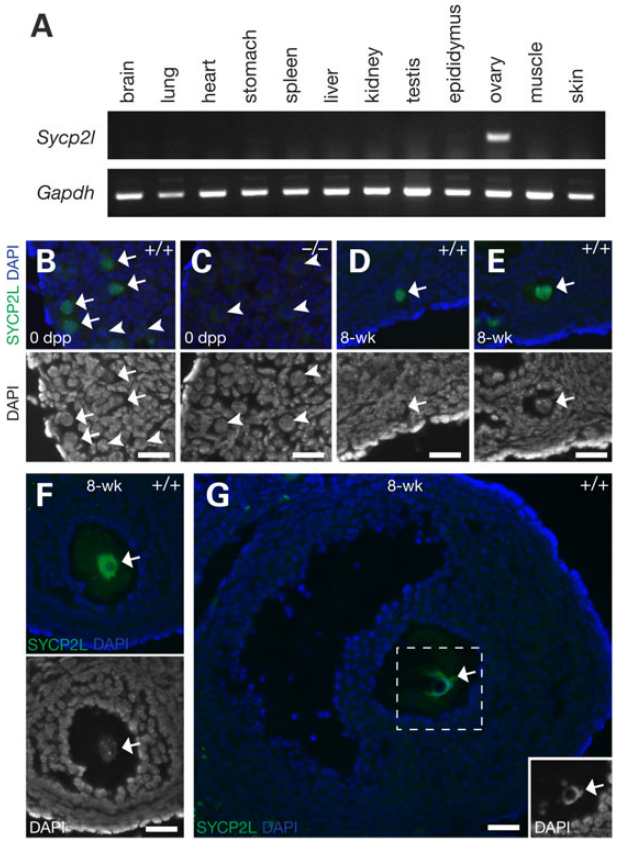

Figure 1. Oocyte-specific expression of mouse SYCP2L. (**A**) RT-PCR analysis of *Sycp2l* expression in adult tissues from 8-week-old mice. *Gapdh* served as a control for a gene with ubiquitous expression. (**B–G**) Nuclear localization of SYCP2L in oocytes. Sectioned ovaries from newborn (0 days postpartum, dpp) (B, wild-type; C, *Sycp2l*$^{-/-}$) and 8-week-old wild-type mice (D–G) were immunostained with anti-SYCP2L antibody. DNA was stained with DAPI. Bottom images in panels B–F and the inset in panel G show nuclear staining only. Arrows and arrowheads mark oocytes with SYCP2L-positive and -negative nuclei, respectively. Note the absence of SYCP2L in the *Sycp2l*-deficient oocyte nuclei (C). In wild-type ovaries, SYCP2L protein was present in the nuclei of newborn oocytes (B), and oocytes from primordial (D), primary (E), secondary (F) and antral follicles (G). Scale bars, 25 μm.

Results

SYCP2L is an oocyte-specific sequence homologue of SYCP2

We determined the mouse full-length *Sycp2l* cDNA sequence by cloning and sequencing. Mouse *Sycp2l* encodes a protein of 842 amino acids (aa) with homology to the SC protein SYCP2 (21,22). The N-terminal (aa 1–382) and C-terminal regions (aa 747–823) of SYCP2L exhibit 39 and 31% sequence identity to SYCP2, respectively, whereas the central region lacks homology. We evaluated *Sycp2l* expression in adult tissues and found that *Sycp2l* is ovary-specific; the transcript was only detected in ovary but not in other adult tissues including testis (Fig. 1A).

To elucidate its putative function in oogenesis, we disrupted the *Sycp2l* gene by homologous recombination in embryonic stem (ES) cells (Supplementary Material, Fig. S1A). Western blot analysis showed that the SYCP2L protein with an apparent molecular weight of ~110 kDa was present in wild-type ovaries but absent in *Sycp2l*$^{-/-}$ ovaries (Supplementary Material, Fig. S1B). We next examined expression and subcellular localization of SYCP2L in the mouse ovary by immunostaining. In newborn ovaries, a small fraction of oocytes remain at the pachytene stage of meiosis I, but most have advanced to the diplotene stage. In wild-type newborn ovaries, SYCP2L was expressed in the majority of oocytes and absent from a subset (Fig. 1B). No immunostaining was observed in oocytes from the *Sycp2l*$^{-/-}$ ovary, validating the specificity of the SYCP2L antibody (Fig. 1C and Supplementary Material, Fig. S1C). In adult wild-type ovaries, SYCP2L was detected in oocytes in primordial follicles (Fig. 1D), primary follicles (Fig. 1E), secondary follicles (Fig. 1F) and antral follicles (Fig. 1G). Consistently, SYCP2L localized to the nucleus of oocytes. These results showed that mouse SYCP2L is an oocyte-specific nuclear protein.

Temporal localization of SYCP2L to the SC

Given that SYCP2 is a component of the SC lateral elements, we performed immunofluorescence analysis of spread nuclei of oocytes from embryonic and newborn ovaries to assess whether SYCP2L localizes to the SC (Fig. 2). The axial elements of SC begin to form along the core of each chromosome at the leptotene stage of meiosis I. At the zygotene stage, synapsis is initiated between homologous chromosomes. At the pachytene stage, all

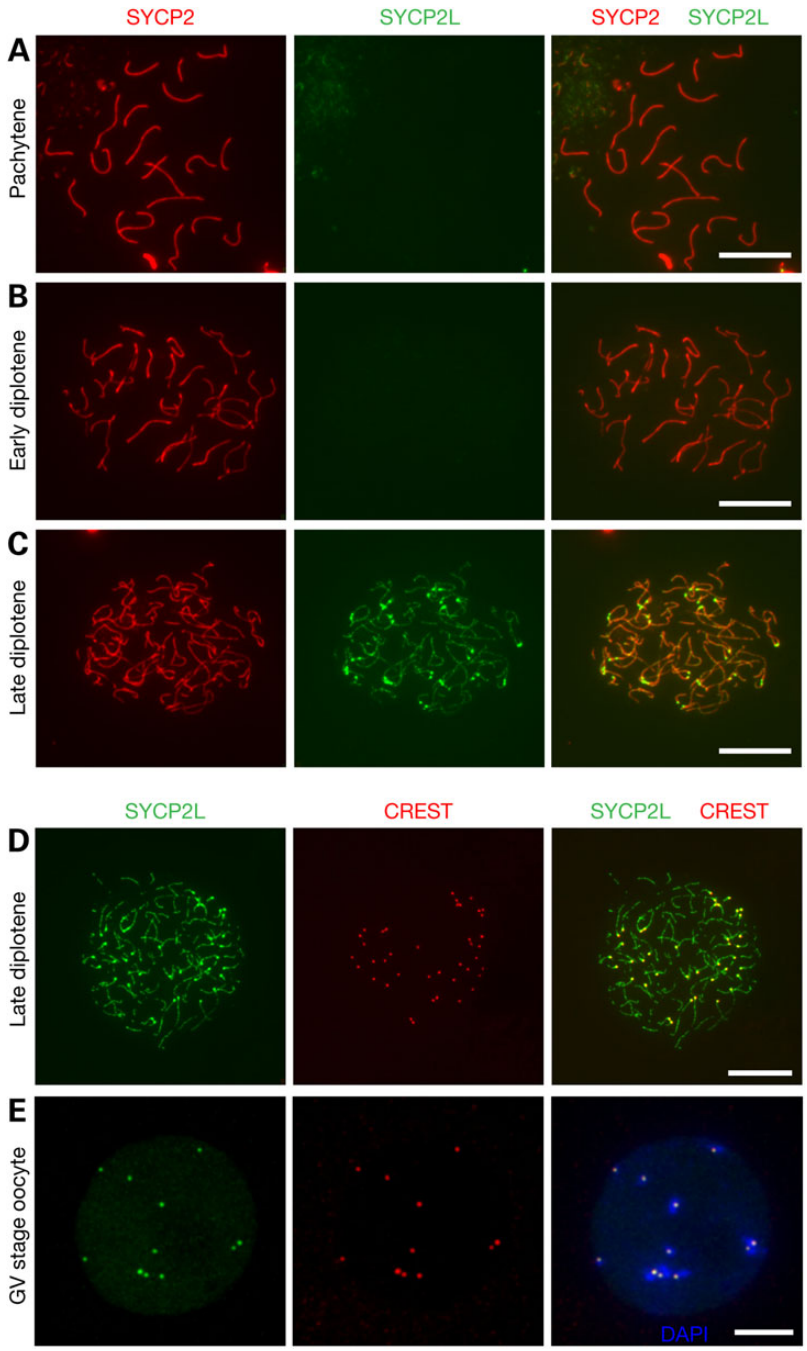

Figure 2. Mouse SYCP2L localizes to SCs and centromeres in late diplotene oocytes at birth. Nuclear spreads of oocytes from newborn mice were immunostained with anti-SYCP2 and anti-SYCP2L antibodies. SYCP2L signal was absent in pachytene (**A**) and early diplotene stage (**B**) oocytes, but present at late diplotene (**C**). (**D**, **E**) Co-immunostaining of oocyte nuclear spreads with anti-SYCP2L antibody and CREST antiserum reveals centromere localization of SYCP2L in late diplotene stage oocyte from newborn ovaries (D) and GV stage oocytes from adult ovaries (E). Scale bars, 10 μm.

homologous chromosomes are fully synapsed. At the subsequent diplotene stage, homologous chromosomes undergo desynapsis, characterized by progressive separation of the SC lateral elements. SYCP2L was absent on the SC of leptotene, zygotene, pachytene and early diplotene oocytes (Fig. 2A and B; Supplementary Material, Fig. S2). Strikingly, SYCP2L localized to the SC lateral elements in late diplotene oocytes (Fig. 2C). These results were consistent with the expression of SYCP2L in some but not all oocytes in the newborn ovary (Fig. 1B). Therefore, the expression of SYCP2L appears to be stage-specific with an onset at the late diplotene stage.

Localization of SYCP2L to centromeres in dictyate oocytes

In addition to its localization to the SC lateral elements, the SYCP2L signal existed as a pair of bright dots at one end of the lateral elements (Fig. 2C). This pattern indicated that the dots might correspond to centromeres, which in mouse are located close to

telomeres. CREST autoimmune serum stains centromeres (34). Double immunostaining of diplotene (i.e. dictyate) oocyte spread nuclei with anti-SYCP2L antibody and CREST confirmed a centromere localization of SYCP2L (Fig. 2D), which was also found in GV (germinal vesicle) stage oocytes from adult ovary (Fig. 2E). In bovine GV stage oocytes, SYCP2L localizes to dot-like structures in the nucleus, and given our results, these dot-like structures in bovine oocytes likely represent centromeres (33).

Centromere localization of ectopically expressed SYCP2L in somatic cells

SYCP2L is not expressed in somatic tissues (Fig. 1A). We ectopically expressed mouse SYCP2L in NIH 3T3 cells. Interestingly, mouse SYCP2L localized to centromeres in NIH 3T3 cells (Supplementary Material, Fig. S3). Furthermore, ectopically expressed human SYCP2L also localized to centromeres in somatic cells such as HEK 293T cells (Fig. 3). Because an intronic single nucleotide polymorphism (SNP) in human *SYCP2L* is associated with ANM, we asked whether non-synonymous SNPs in human *SYCP2L* might affect protein function. Specifically, we examined the effect of human non-synonymous SNPs in *SYCP2L* on centromere localization of the corresponding mutant SYCP2L proteins in transfected 293T cells. We selected missense SNPs with a minor allele frequency of >0.01. From the NCBI SNP database, we identified three missense SNPs that meet this cutoff (Fig. 3A). We also included two SNPs that introduce a stop codon, although their allele frequency is very low (Fig. 3A). All five human SYCP2L mutant proteins were expressed in 293T cells after transfection with expression constructs (Fig. 3B). Immunostaining revealed that the three mutant protein variants with missense SNPs (mutants 1–3) were localized to centromeres (Fig. 3C). In contrast, the two truncated SYCP2L mutants (mutants 4 and 5) were not specifically localized to the centromeres but distributed diffusely throughout the nucleus (Fig. 3C), suggesting that the C-terminal region of SYCP2L is required for its centromere localization. These results indicate that the rare nonsense SNPs in human SYCP2L may alter the protein distribution and thereby function.

Human *SYCP2L* intronic SNP rs2153157 affects U12-type intron splicing

GWAS studies have shown that the A allele of human *SYCP2L* SNP rs2153157 (A/G) is associated with later ANM (5) and this association was confirmed in an independent GWAS study (8). SNP rs2153157 is located in intron 4 of human *SYCP2L* gene (Fig. 4A). This intron has AT-AC terminal dinucleotides and represents a U12-type intron (Fig. 4A). Most introns contain GT-AG terminal dinucleotides and are therefore U2 type, whereas U12-type introns are rare, accounting for less than 0.5% of all introns (35,36). U12-type introns are processed by the minor spliceosome, which is distinct from the U2-dependent major spliceosome (36). U12-type introns are spliced less efficiently than U2 introns, and it has been postulated that the slower splicing rate of U12 introns limits the expression level of genes harboring such introns (37).

To test whether the A or G allele of SNP rs2153157 affects splicing of the U12-type intron, we used an exon trap approach (Fig. 4A). This construct contained a fragment encompassing

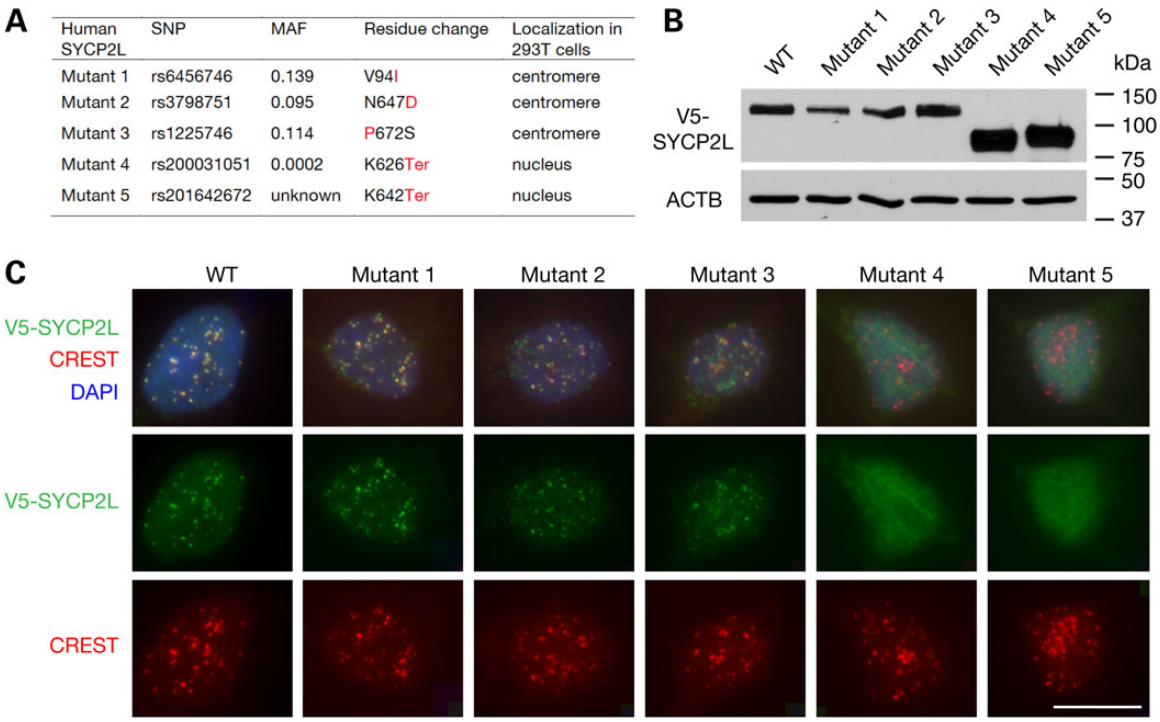

Figure 3. Ectopically expressed human SYCP2L localizes to centromeres in 293T cells. (**A**) Properties of five human SYCPL2 proteins resulting from SNPs. Three SNPs result in a missense mutation, and two SNPs cause a termination codon leading to C-terminal truncation. There are only three missense SNPs with a minor allele frequency (MAF) of >0.01 in human *SYCP2L* gene. Corresponding minor allele residues or termination codons are shown in red. (**B**) Western blot analysis of human SYCP2L mutants in transfected 293T cells. V5-SYCP2L protein variants were detected using an anti-V5 tag antibody; ACTB served as a loading control. (**C**) Localization of wild-type and mutant human SYCP2L variants in transfected 293T cells. V5-SYCP2L protein and centromeres were identified by immunostaining with an anti-V5 antibody and CREST antiserum, respectively (also shown in separate channels). DNA was stained with DAPI. Scale bar, 20 μm.

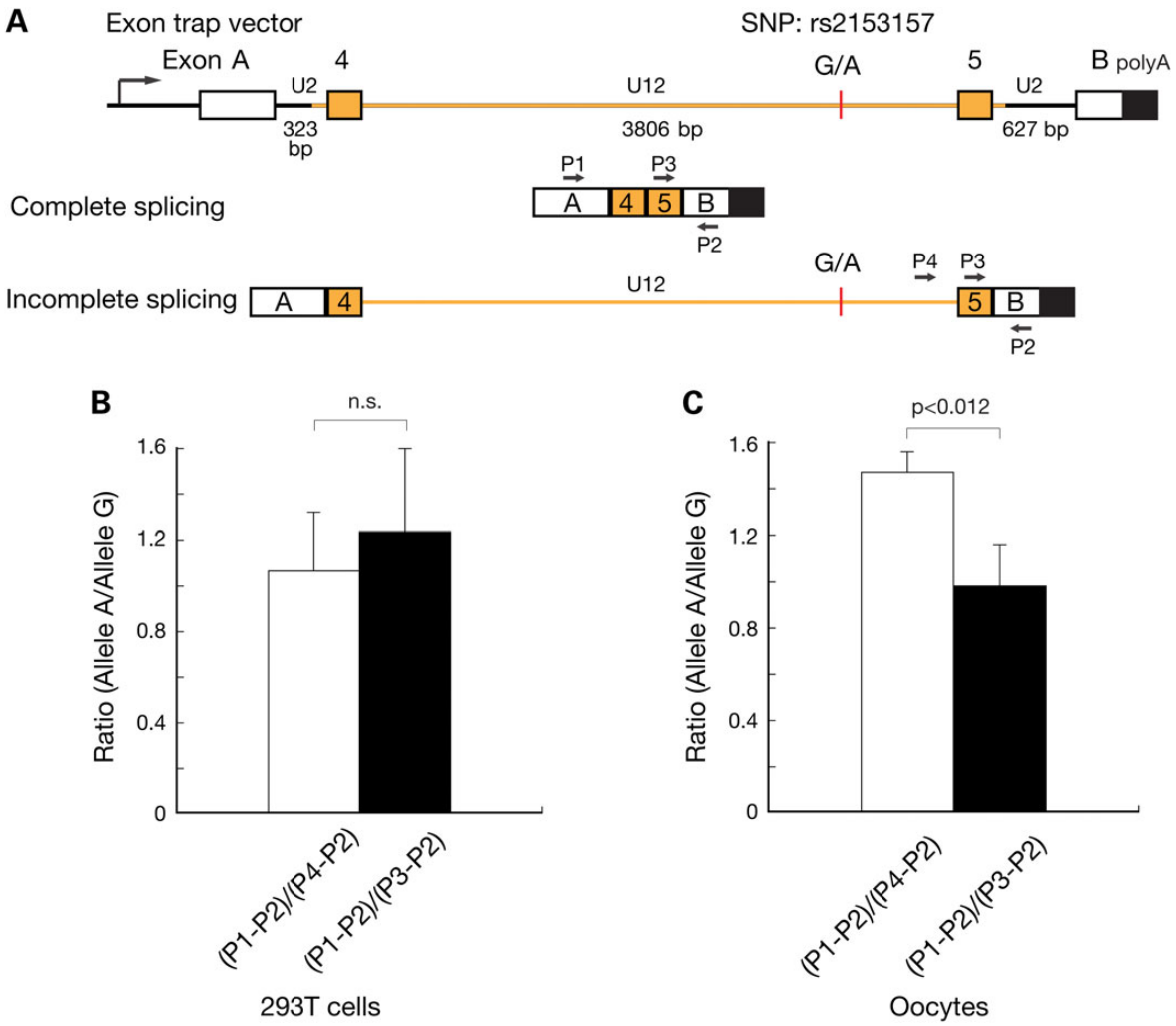

Figure 4. Effect of human *SYCP2L* SNP rs2153157 on splicing efficiency. (**A**) Schematic diagram of the exon trap construct. Exons A and B are from the backbone exon trap vector. Exons 4 and 5 from human *SYCP2L* gene are depicted. Human *SYCP2L* intron 4 (in orange) is a U12 intron and harbors the SNP rs2153157. The other two introns in the construct are U2 introns. Two versions of the construct were generated, containing either G or A in the U12 intron. The minor allele frequency (G-allele) in human population is 0.4201. Completely spliced and partially spliced transcripts are shown schematically along with the position of PCR primers (P1-P4). The size of the introns is shown. (**B**) SNP rs2153157 does not affect splicing efficiency in somatic 293T cells. The splicing rate of U12 introns is several fold lower than that of U2 introns (37). PCR with primers P1 and P2 only amplifies completely spliced transcript, whereas PCR with primers P4 and P2 amplifies only an incompletely spliced transcript containing the U12-type intron 4. Primers P3 and P2 amplify both transcripts. The (P1-P2)/(P4-P2) PCR product ratio uses the U12-type splicing as the reference, whereas the (P1-P2)/(P3-P2) uses the U2-type splicing as the reference. (**C**) Increased splicing efficiency of the SNP rs2153157 A allele in 12 dpp mouse oocytes.

intron 3 to intron 5 of human *SYCP2L*, including intron 4 and its flanking exons 4 and 5; additionally, two U2-type introns were present on either side that linked the *SYCP2L* sequence to upstream and downstream exons of the vector sequence. By RT-PCR with primers specific for the vector-encoded exons, *SYCP2L* exon 5 and intron 4 downstream of SNP rs2153157, we determined ratios between completely spliced and partially spliced transcripts. Specifically, we compared two ratios: the ratio between completely processed transcripts (fragment produced by PCR with primers 1 and 2, P1-2) and incompletely processed transcript with a remaining U12-type intron 4 (P4-P2), and the ratio of completely spliced transcript (P1-P2) and any complete or partially spliced transcripts lacking the U2-type intron downstream of SNP rs2153157 (P3-P2; Fig. 4A). These ratios therefore reflect the splicing efficiency of U12- and U2-type introns, respectively.

We first transfected HEK 293T cells with either one of two exon trap vector constructs containing the G and A alleles of SNP rs2153157, respectively. Quantitation assays showed that in 293T cells, the splicing efficiency was similar between the two alleles (Fig. 4B). We next injected each construct into transcription-competent mouse oocytes collected from postnatal day 12 ovaries (Fig. 4C). The (P1-P2)/(P3-P2) PCR product ratio was similar between alleles A and G, indicating similar splicing efficiency of the U2 intron (Fig. 4C). In contrast, the (P1-P2)/(P4-P2) ratio was significantly higher for the A versus the G allele, suggesting that in oocytes, the U12 intron is more efficiently spliced when the A allele is present compared with the G allele (Fig. 4C). Therefore, the two alleles of intronic SNP rs2153157 had different effects on the efficiency of U12 intron splicing in oocytes but not in 293T somatic cells. Such an oocyte-specific splicing effect may be attributed to differential expression of minor spliceosome components between oocytes and somatic tissues. It is also possible that SNP rs2153157 may be located in an oocyte-specific splicing enhancer or repressor.

SYCP2L-deficient females exhibit age-associated progressive loss of oocytes

Consistent with the lack of *Sycp2l* expression in testis (Fig. 1A), *Sycp2l*$^{-/-}$ males were fertile with normal testis weight (*Sycp2l*$^{-/-}$, 189 ± 27 mg; wild-type/*Sycp2l*$^{+/-}$, 180 ± 11 mg) and normal sperm count (*Sycp2l*$^{-/-}$, 2.2 ± 0.5 × 10^7; wild-type/*Sycp2l*$^{+/-}$, 2.1 ± 0.4 × 10^7). Immunostaining for STK31, a protein specifically expressed in the cytoplasm of germ cells, revealed that oocytes were present in the ovaries of *Sycp2l*$^{-/-}$ mice at 10 days postpartum (dpp) (Supplementary Material, Fig. S1C) (38,39). We quantified the number of oocytes in ovaries of female mice from 10 dpp to 14 months and found a progressive reduction in their number in *Sycp2l*$^{-/-}$ females relative to control females (wild-type and *Sycp2l*$^{+/-}$) over time (Fig. 5A). Notably, at 10 dpp, oocyte numbers were similar between *Sycp2l*$^{-/-}$ and control females (Fig. 5A, B); however, at 14 months, the number of oocytes in *Sycp2l*$^{-/-}$ female mice was only 20% of that in control females (Fig. 5A).

We further quantified oocytes by follicular stage, including primordial, primary, secondary and antral follicles. At 10 dpp, the number of primordial follicles was similar between *Sycp2l*$^{-/-}$ and control females, suggesting that formation of the initial reserve pool of oocytes was not affected in *Sycp2l*$^{-/-}$ females (Fig. 5B). At 2 months and 8 months, the number of primordial follicles was significantly reduced in *Sycp2l*$^{-/-}$ females compared with controls, whereas the number of developing (primary, secondary and antral) follicles was similar between *Sycp2l*$^{-/-}$ and control females (Fig. 5C, D). At 12 months, the number of primordial follicles was further reduced in *Sycp2l*$^{-/-}$ females, and strikingly, the number of primary and secondary follicles was also significantly lower in *Sycp2l*$^{-/-}$ females than in control females (Fig. 5E). This reduction in the number of primordial, primary and secondary follicles persisted in *Sycp2l*$^{-/-}$ females at 14 months (Fig. 5F). In conclusion, the initial pool of primordial follicles was established normally in *Sycp2l*$^{-/-}$ females; however, primordial follicles were progressively lost with increasing age, leading to a significant reduction in the number of primary and secondary follicles in mice at advanced ages. These results suggest that SYCP2L plays an important role in the survival of primordial oocytes.

Reduced fertility in SYCP2L-deficient females

We assessed the fertility of *Sycp2l*$^{-/-}$ females by mating tests starting at 6 weeks of age (Table 1). Before the age of 8 months, *Sycp2l*$^{-/-}$ females produced the same number of litters but a lower total number of pups compared with control females; the litter size of *Sycp2l*$^{-/-}$ females was lower. Both control and *Sycp2l*$^{-/-}$ females became less fertile with aging: compared with the litter size produced before the age of 8 months, the litter size obtained from 8 months to 14 months was significantly lower in both groups (control females, $P < 0.0001$; *Sycp2l*$^{-/-}$ females, $P < 0.0001$). In comparison with control females, *Sycp2l*$^{-/-}$

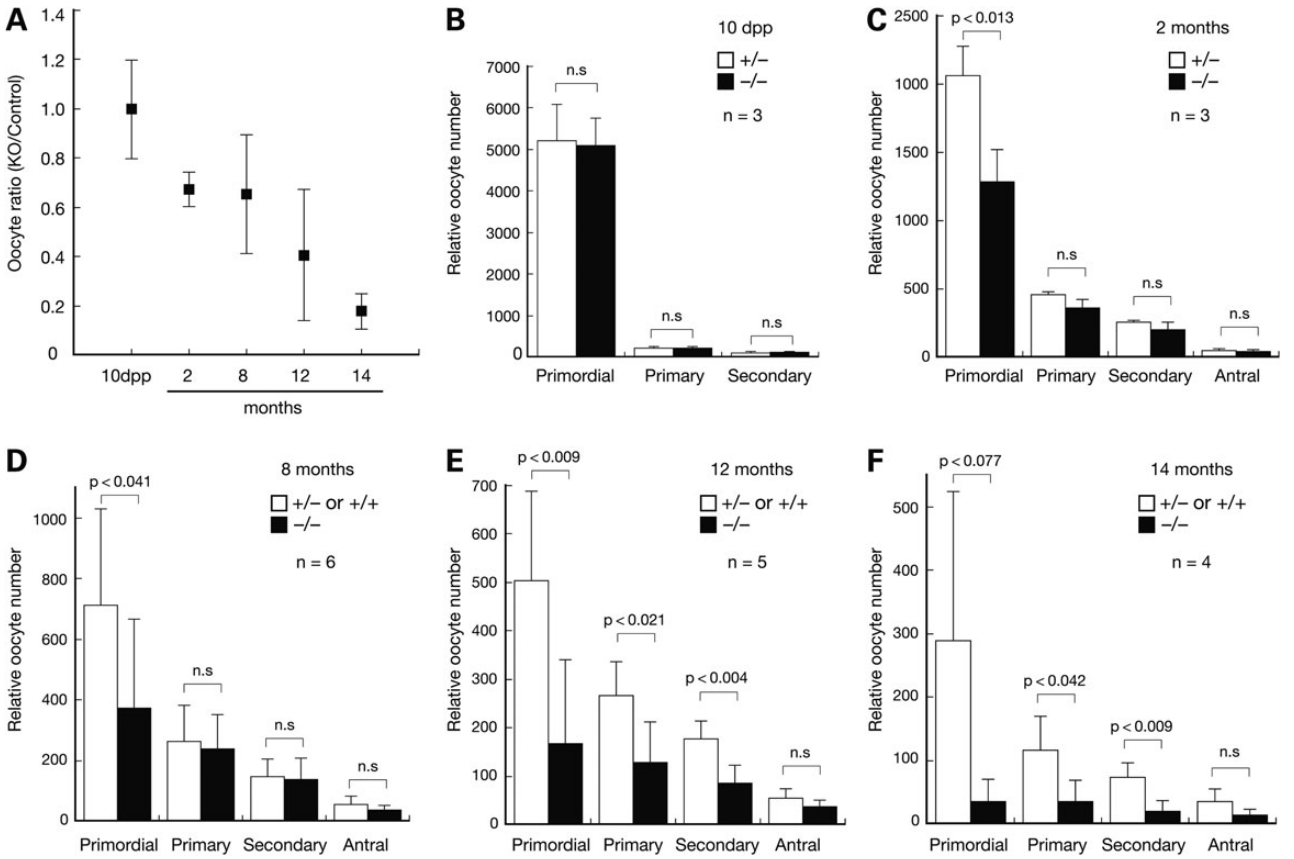

Figure 5. Age-associated reduction of oocyte number in *Sycp2l*$^{-/-}$ females. For each mouse, serial sections of one ovary were prepared and follicles containing an oocyte with visible nucleus counted in every fifth section. The sum of oocytes from all counted sections was considered the total number of oocytes per ovary. (**A**) Progressive loss of oocytes in *Sycp2l*$^{-/-}$ females with age. Control genotypes included *Sycp2l*$^{+/-}$ and wild-type. (**B–F**) Oocyte counts in ovaries from females at 10 dpp (B), 2 months (C), 8 months (D), 12 month (E) and 14 months of age (F). *n*, number of mice per genotype. *P*-values for Student's *t*-Test are shown. n.s., not significant.

Table 1. Fecundity of *Sycp2l*$^{-/-}$ and control females

Genotype	6 weeks–8 months			8–14 months		
	+/+ or +/–	–/–	*P*-value	+/+ or +/–	–/–	*P*-value
Pups/cage[a]	139.3 ± 24.4	122.3 ± 14.0	0.35	52.7 ± 6.8	29.3 ± 4.0	0.007*
Litters/cage	15.7 ± 1.2	15.7 ± 1.5	1.00	10.3 ± 3.1	8.0 ± 1.0	0.28
Litter size	8.9 ± 2.6	7.8 ± 2.4	0.039*	5.1 ± 2.8	3.7 ± 2.3	0.047*

[a]Each cage housed one male and two females, starting out with 6-week-old females. Per group, three cages were assessed until females reached the age of 14 months.
*Significantly different per Student's *t*-Test.

females older than 8 months of age produced a similar number of litters; however, litters were much smaller, resulting in a significantly lower number of offspring. To determine if differences in hormone levels were associated with these observations, we measured blood levels of follicle-stimulating hormone (FSH) and luteinizing hormone (LH) in female mice at 8 months, 12 months and 14 months of age. The levels of both FSH and LH were similar between *Sycp2l*$^{-/-}$ and control females at all time points (Supplementary Material, Fig. S4), ruling out insufficient hormonal stimulation as a primary cause for the reduced fertility of *Sycp2l*$^{-/-}$ females. The reduced fertility in aged *Sycp2l*$^{-/-}$ females was, however, consistent with and likely caused by the severe oocyte loss observed in mutant females.

Intact DNA damage checkpoint in SYCP2L-deficient oocytes

The oocyte DNA damage checkpoint pathway ensures that meiotic oocytes with unrepaired DNA damage undergo apoptosis (40,41). When the DNA damage checkpoint is disabled, oocytes do not die, even in the presence of extensive DNA damage. TAp63, a p63 isoform, is a nuclear protein and is specifically expressed in meiotically arrested oocytes. TAp63 is required for DNA damage-induced apoptosis of primordial oocytes (42,43). Because, like TAp63, SYCP2L is also an oocyte-specific nuclear protein with abundant expression in primordial follicles, we next examined if SYCP2L was also a necessary component of the DNA damage response in oocytes. We exposed *Sycp2l*$^{+/-}$ and *Sycp2l*$^{-/-}$ females at 5 dpp to 0.45 Gy of γ-irradiation to induce DNA damage and assessed for the presence of oocytes at 10 dpp by immunostaining with an antibody against the germ cell-specific RNA binding protein MSY2 (44). Both *Sycp2l*$^{+/-}$ and *Sycp2l*$^{-/-}$ ovaries were depleted of primordial oocytes upon γ-irradiation, suggesting that SYCP2L is not required for the DNA damage checkpoint in oocytes.

Discussion

In this study, we demonstrate that SYCP2L is specifically expressed in oocytes, localizes to centromeres at the dictyate stage, and regulates the survival of primordial oocytes. Disruption of *Sycp2l* accelerates the age-associated decline of fertility in female mice. Our results strongly support the association of human SYCP2L locus with ANM in women (5,8). The question arises as to the function of SYCP2L at the centromeres. SC proteins such as SYCP1 and SYCP3 persist at centromeres after their disassembly from the lateral elements in diplotene spermatocytes (45,46). It has been hypothesized that these retained SYCP proteins play a role in the maintenance of centromere association, organization of chiasmata and assembly of kinetochores in preparation for bi-orientation and faithful segregation of homologous chromosomes in mammalian spermatocytes. The oocyte dictyate (diplotene) stage spans from birth to ovulation, lasting for up to four decades in women. SYCP2L localizes to centromeres in oocytes and thus might be involved in the local chromatin organization around centromeres. Although SYCP2L is not required for the DNA damage checkpoint, it might still play a role in sensing and repairing DNA damage to promote the survival of oocytes.

Human GWAS studies have shown that the A allele of SYCP2L intronic SNP rs2153157 is associated with later ANM (5,8). Here we demonstrate that in oocytes, the A allele is spliced more efficiently than the G allele, and thus expressed at a higher level. Therefore, our splicing data support the human GWAS study and provide a possible molecular explanation for the effect of this intronic SNP on ANM.

SYCP2L is a sequence paralogue of SYCP2; however, expression, localization and function of these two homologues are strikingly different. *Sycp2* is expressed in both testis and ovary and is essential for male fertility (22). In contrast, *Sycp2l* is restricted to the ovary and not expressed in the testis, such that deficiency of *Sycp2l* does not affect male fertility. In germ cells of both sexes, SYCP2 is essential for assembly of SCs and incorporation of SYCP3 into lateral/axial elements (22). Disruption of SYCP2 function results in a sexually dimorphic phenotype: male mice expressing a mutant form of SYCP2 lacking the SYCP3 binding domain are sterile, due to meiotic arrest following a failure in synapsis, whereas *Sycp2* mutant females are subfertile (22). The subfertility phenotype of *Sycp2* mutant females is much more severe than that of *Sycp2l*-deficient females and has an earlier onset. *Sycp2* mutant females have significantly reduced litter sizes as early as at 8 weeks, whereas *Sycp2l*-deficiency associated subfertility becomes fully apparent only in aged females (22). The earlier onset of reduced fertility in *Sycp2* mutant females is consistent with the key role of SYCP2 during SC assembly. Because of the expression of SYCP2L in late diplotene oocytes, the absence of a profound early-onset infertility or subfertility phenotype in females is not surprising. Furthermore, both SYCP2L and SYCP2 localize to the SC lateral elements in late diplotene oocytes; therefore, SYCP2 may partially compensate for some aspects of SYCP2L function in *Sycp2l*$^{-/-}$ females.

Sequence paralogues have been identified for another SC protein—SYCP3. In mouse, multi-copy *Sycp3*-like genes exist on the X and Y chromosomes (called *Slx/Slx1* and *Sly* respectively) (47–50). *Sycp3*-like genes function in post-meiotic male germ cells rather than in meiotic germ cells. The *Sly* gene family represses the transcription of XY genes post-meiotically in the male germ cells, whereas *Slx/Slx1* stimulates the expression of XY genes, providing genetic evidence for the concept that the amplification of *Sycp3*-like genes on the X and Y chromosomes plays antagonistic roles in the intragenomic conflict between the X and Y chromosomes in post-meiotic germ cells (49). Apparently, both *Sycp2*-like and *Sycp3*-like genes have evolved toward new and different roles in gametogenesis.

Materials and Methods

Cloning of mouse and human full-length *Sycp2l* cDNA sequences

Fragments encompassing the 5′ and 3′ portions of mouse *Sycp2l* cDNA were amplified from C57BL/6J mouse ovary total RNA by RT-PCR. The full-length cDNA was obtained by overlapping PCR, inserted into the expression vector pcDNA3.1/V5-His, and sequenced. The mouse *Sycp2l* mRNA sequence was deposited in GenBank (accession no. KP872825). The 5′ and 3′ fragments of human *SYCP2L* cDNA were amplified from human ovary cDNA pool (BD Biosciences Clontech) and a *SYCP2L* cDNA clone (accession no. BC012225), respectively, followed by overlapping PCR to obtain the full-length human *SYCP2L* cDNA.

Antibody production

A 6xHis-SYCP2L (mouse, 1–336 aa) fusion protein was expressed in *E. coli* strain M15 using the pQE30 vector and purified by Ni-NTA resin. The purified protein was used to immunize rabbits at Cocalico Biologicals Inc., resulting in polyclonal antisera UP2395. Affinity purified SYCP2L antibody was used for Western blot and immunofluorescence analyses.

Generation of *Sycp2l* mutant mice

To generate the *Sycp2l* targeting construct, two DNA fragments (2.3 and 2.4 kb) were amplified by high-fidelity PCR using a *Sycp2l*-containing BAC clone (RP23-2H11) as a template (Supplementary Material, Fig. S1A). Hybrid V6.5 ES cells (C57BL/6 × 129/sv) were electroporated with linearized targeting construct (pJZ84/*ClaI*) and were cultured in the presence of G418 (350 μg/ml; Gibco) and gancyclovir (2 μM; Sigma) (51). Screening 192 drug-resistant ES cell clones identified eight homologously targeted clones. Two clones (1D7 and 2G10) were injected into C57BL/6 × C3H F1 (B6C3F1; Taconic) blastocysts. The offspring were genotyped by PCR using primers GACAACAGCCAGTCCTCAGAAAC and GGGTTCACAAGGCTCCACTG specific for the wild-type allele (471 bp), and primers GCATATGGGCTCTATGGTTAAGA and CCTACCGGTGGATGTGGAATGTGTG for the *Sycp2l* knockout allele (400 bp).

Western blot analyses

Eight to ten pairs of ovaries for each genotype were collected from 10-day-old pups, homogenized in 50 μl of SDS-PAGE sample buffer and heated at 95°C for 5 min. From each sample, 20 μl of total protein extract was resolved on 10% SDS-PAGE gel and electroblotted onto nitrocellulose membranes using iBlot (Invitrogen). The primary antibodies were anti-SYCP2L antibody UP2395 (1:50), V5 antibody (1:5000, Invitrogen) and ACTB antibody (1:8000, Sigma).

Immunofluorescence and nuclear surface spread analyses

For immunofluorescence, ovaries were fixed in 4% PFA for 3 h at 4°C, dehydrated in 30% sucrose solution overnight and sectioned using a cryostat. 293T cells on slides were fixed with 4% PFA for 5 min at room temperature. GV oocytes were fixed in 2% PFA for 20 min at room temperature. Surface spreads of oocyte nuclei were performed as described previously (52). For nuclear spread analysis, oocytes were retrieved from embryonic day 15.5 (E15.5), E18.5 and newborn ovaries. The primary antibodies used for immunofluorescence were: anti-SYCP2L UP2395 (1:10), anti-SYCP2 serum GP21 (1:100) (22), CREST antiserum (1:5000, a gift from B.R. Brinkley) (34), anti-V5 antibody (1:1000, Invitrogen) and anti-STK31 GP79 (1:20) (39).

Mating test

Mating cages housing two females and one healthy wild-type 2-month-old male per cage were set up when female mice were 6 weeks of age; with a total of six females per group (*Sycp2l*$^{-/-}$ and *Sycp2l*$^{+/-}$/*Sycp2l*$^{+/+}$). Cages were observed daily and litter sizes recorded until the females reached the age of 14 months.

Splicing assays in 293T cells and oocytes

A DNA fragment encompassing the sequence from intron 3 to intron 5 of the human *SYCP2L* gene was amplified from the BAC clone RP11-637O19 (which contains the G allele) by high-fidelity PCR and the fragment was subcloned into the exon trap vector pET01 using the XhoI and NotI restriction sites (Fig. 4A). The A allele was generated by PCR-mediated mutagenesis as described previously (53). The plasmids were transfected into 293T cells using lipofectamine 2000 (Invitrogen) followed by extraction of total RNA using TRIzol reagent (Invitrogen) at 24 h post transfection. For each construct, three independent transfections were performed. Oocytes from 12-day-old mice were microinjected with 10 000 copies of the plasmid per oocyte. For each construct, three separate injection experiments involving 20–30 oocytes were performed. Total RNA from oocytes was isolated using Arcturus′ PicoPure RNA isolation kit. Reverse transcription primed with random hexamers was performed using 0.5 μg of total RNA from transfected 293 T cells or microinjected oocytes per reaction. Products were amplified using a limited number of PCR cycles such that product saturation was not reached, separated by electrophoresis and quantified using ImageQuant software.

Hormone measurements

Blood samples collected from female mice at the age of 8, 12 and 14 months were allowed to clot at room temperature for 90 min, followed by isolation of serum by centrifugation at 2000g for 15 min. Mouse FSH and LH assays were performed at the University of Virginia School of Medicine Center for Research in Reproduction Ligand Assay and Analysis Core.

Follicle quantification

Quantification of mouse oocyte number was performed as previously described (54). Ovaries from 10-day- and 2-, 8-, 12- and 14-month-old mice were fixed in Bouin's solution overnight, dehydrated, embedded in paraffin, sectioned at 8-μm intervals and stained with hematoxylin and eosin. For each mouse, the number of follicles was counted in every fifth section of one ovary, and the sum of oocytes from all counted sections was considered the total number of oocytes per ovary. Only those oocytes with a visible nucleus were counted to avoid duplicate count. Oocyte stages were identified as follows. In primordial follicles, the oocyte is surrounded by flattened granulosa cells. In primary follicles, the oocyte is surrounded by a single layer of cuboidal granulosa cells. Secondary follicles contain more than one layer of cuboidal granulosa cells without a visible antrum. Antral follicles contain antral space within granulosa cell layers.

Supplementary Material

Supplementary Material is available at *HMG* online.

Acknowledgements

We thank B.R. Brinkley for CREST antiserum, S. Eckardt for help with manuscript preparation and F. Yang for providing embryonic oocyte samples.

Conflict of Interest statement. None declared.

Funding

This work was supported by National Institutes of Health/National Institute of General Medical Sciences (Grant number GM089893 and GM076327 to P.J.W.). The University of Virginia Center for Research in Reproduction Ligand Assay and Analysis Core is supported by the Eunice Kennedy Shriver NICHD/NIH (SCCPIR) Grant U54-HD28934.

References

1. Cooper, G.S. and Sandler, D.P. (1998) Age at natural menopause and mortality. *Ann. Epidemiol.*, **8**, 229–235.
2. Wellons, M., Ouyang, P., Schreiner, P.J., Herrington, D.M. and Vaidya, D. (2012) Early menopause predicts future coronary heart disease and stroke: the multi-ethnic study of atherosclerosis. *Menopause*, **19**, 1081–1087.
3. Lindquist, O., Bengtsson, C., Hansson, T. and Roos, B. (1979) Age at menopause and its relation to osteoporosis. *Maturitas*, **1**, 175–181.
4. Hsieh, C.C., Trichopoulos, D., Katsouyanni, K. and Yuasa, S. (1990) Age at menarche, age at menopause, height and obesity as risk factors for breast cancer: associations and interactions in an international case-control study. *Int. J. Cancer*, **46**, 796–800.
5. He, C., Kraft, P., Chen, C., Buring, J.E., Pare, G., Hankinson, S.E., Chanock, S.J., Ridker, P.M., Hunter, D.J. and Chasman, D.I. (2009) Genome-wide association studies identify loci associated with age at menarche and age at natural menopause. *Nat. Genet.*, **41**, 724–728.
6. Stolk, L., Zhai, G., van Meurs, J.B., Verbiest, M.M., Visser, J.A., Estrada, K., Rivadeneira, F., Williams, F.M., Cherkas, L., Deloukas, P. *et al.* (2009) Loci at chromosomes 13, 19 and 20 influence age at natural menopause. *Nat. Genet.*, **41**, 645–647.
7. Stolk, L., Perry, J.R., Chasman, D.I., He, C., Mangino, M., Sulem, P., Barbalic, M., Broer, L., Byrne, E.M., Ernst, F. *et al.* (2012) Meta-analyses identify 13 loci associated with age at menopause and highlight DNA repair and immune pathways. *Nat. Genet.*, **44**, 260–268.
8. Carty, C.L., Spencer, K.L., Setiawan, V.W., Fernandez-Rhodes, L., Malinowski, J., Buyske, S., Young, A., Jorgensen, N.W., Cheng, I., Carlson, C.S. *et al.* (2013) Replication of genetic loci for ages at menarche and menopause in the multi-ethnic population architecture using genomics and epidemiology (PAGE) study. *Hum. Reprod.*, **28**, 1695–1706.
9. Chen, C.T., Liu, C.T., Chen, G.K., Andrews, J.S., Arnold, A.M., Dreyfus, J., Franceschini, N., Garcia, M.E., Kerr, K.F., Li, G. *et al.* (2014) Meta-analysis of loci associated with age at natural menopause in african-american women. *Hum. Mol. Genet.*, **23**, 3327–3342.
10. AlAsiri, S., Basit, S., Wood-Trageser, M.A., Yatsenko, S.A., Jeffries, E.P., Surti, U., Ketterer, D.M., Afzal, S., Ramzan, K., Faiyaz-Ul Haque, M. *et al.* (2015) Exome sequencing reveals MCM8 mutation underlies ovarian failure and chromosomal instability. *J. Clin. Invest.*, **125**, 258–262.
11. Nishimura, K., Ishiai, M., Horikawa, K., Fukagawa, T., Takata, M., Takisawa, H. and Kanemaki, M.T. (2012) Mcm8 and Mcm9 form a complex that functions in homologous recombination repair induced by DNA interstrand crosslinks. *Mol. Cell*, **47**, 511–522.
12. Lutzmann, M., Grey, C., Traver, S., Ganier, O., Maya-Mendoza, A., Ranisavljevic, N., Bernex, F., Nishiyama, A., Montel, N., Gavois, E. *et al.* (2012) MCM8- and MCM9-deficient mice reveal gametogenesis defects and genome instability due to impaired homologous recombination. *Mol. Cell*, **47**, 523–534.
13. McCarrey, J.R. (1993) Development of the germ cell. In Desjardins, C. and Ewing, L. (eds), *Cell and Molecular Biology of the Testis*. Oxford University Press, New York, Vol. V, pp. 58–89.
14. Handel, M.A. and Schimenti, J.C. (2010) Genetics of mammalian meiosis: regulation, dynamics and impact on fertility. *Nat. Rev. Genet.*, **11**, 124–136.
15. Lesch, B.J. and Page, D.C. (2012) Genetics of germ cell development. *Nat. Rev. Genet.*, **13**, 781–794.
16. Zickler, D. and Kleckner, N. (1999) Meiotic chromosomes: integrating structure and function. *Annu. Rev. Genet.*, **33**, 603–754.
17. Page, S.L. and Hawley, R.S. (2004) The genetics and molecular biology of the synaptonemal complex. *Annu. Rev. Cell Dev. Biol.*, **20**, 525–558.
18. Costa, Y. and Cooke, H.J. (2007) Dissecting the mammalian synaptonemal complex using targeted mutations. *Chromosome Res.*, **15**, 579–589.
19. Yang, F. and Wang, P.J. (2009) The mammalian synaptonemal complex: a scaffold and beyond. *Genome Dyn.*, **5**, 69–80.
20. Schalk, J.A., Dietrich, A.J., Vink, A.C., Offenberg, H.H., van Aalderen, M. and Heyting, C. (1998) Localization of SCP2 and SCP3 protein molecules within synaptonemal complexes of the rat. *Chromosoma*, **107**, 540–548.
21. Offenberg, H.H., Schalk, J.A., Meuwissen, R.L., van Aalderen, M., Kester, H.A., Dietrich, A.J. and Heyting, C. (1998) SCP2: a major protein component of the axial elements of synaptonemal complexes of the rat. *Nucleic Acids Res.*, **26**, 2572–2579.
22. Yang, F., De La Fuente, R., Leu, N.A., Baumann, C., McLaughlin, K.J. and Wang, P.J. (2006) Mouse SYCP2 is required for synaptonemal complex assembly and chromosomal synapsis during male meiosis. *J. Cell Biol.*, **173**, 497–507.
23. Yuan, L., Liu, J.G., Zhao, J., Brundell, E., Daneholt, B. and Hoog, C. (2000) The murine SCP3 gene is required for synaptonemal complex assembly, chromosome synapsis, and male fertility. *Mol. Cell*, **5**, 73–83.
24. Costa, Y., Speed, R., Ollinger, R., Alsheimer, M., Semple, C.A., Gautier, P., Maratou, K., Novak, I., Hoog, C., Benavente, R. *et al.* (2005) Two novel proteins recruited by synaptonemal complex protein 1 (SYCP1) are at the centre of meiosis. *J. Cell. Sci.*, **118**, 2755–2762.
25. Bolcun-Filas, E., Hall, E., Speed, R., Taggart, M., Grey, C., de Massy, B., Benavente, R. and Cooke, H.J. (2009) Mutation of the mouse Syce1 gene disrupts synapsis and suggests a link between synaptonemal complex structural components and DNA repair. *PLoS Genet.*, **5**, e1000393.
26. Bolcun-Filas, E., Costa, Y., Speed, R., Taggart, M., Benavente, R., De Rooij, D.G. and Cooke, H.J. (2007) SYCE2 is required for synaptonemal complex assembly, double strand break repair, and homologous recombination. *J. Cell Biol.*, **176**, 741–747.
27. Schramm, S., Fraune, J., Naumann, R., Hernandez-Hernandez, A., Hoog, C., Cooke, H.J., Alsheimer, M. and Benavente,

R. (2011) A novel mouse synaptonemal complex protein is essential for loading of central element proteins, recombination, and fertility. *PLoS Genet.*, **7**, e1002088.
28. Hamer, G., Gell, K., Kouznetsova, A., Novak, I., Benavente, R. and Hoog, C. (2006) Characterization of a novel meiosis-specific protein within the central element of the synaptonemal complex. *J. Cell. Sci.*, **119**, 4025–4032.
29. Hamer, G., Wang, H., Bolcun-Filas, E., Cooke, H.J., Benavente, R. and Hoog, C. (2008) Progression of meiotic recombination requires structural maturation of the central element of the synaptonemal complex. *J. Cell. Sci.*, **121**, 2445–2451.
30. Tarsounas, M., Pearlman, R.E., Gasser, P.J., Park, M.S. and Moens, P.B. (1997) Protein–protein interactions in the synaptonemal complex. *Mol. Biol. Cell*, **8**, 1405–1414.
31. de Vries, F.A., de Boer, E., van den Bosch, M., Baarends, W.M., Ooms, M., Yuan, L., Liu, J.G., van Zeeland, A.A., Heyting, C. and Pastink, A. (2005) Mouse Sycp1 functions in synaptonemal complex assembly, meiotic recombination, and XY body formation. *Genes Dev.*, **19**, 1376–1389.
32. de Boer, E. and Heyting, C. (2006) The diverse roles of transverse filaments of synaptonemal complexes in meiosis. *Chromosoma*, **115**, 220–234.
33. Voltmer-Irsch, S., Kneissel, S., Adenot, P.G. and Schmidt-Zachmann, M.S. (2007) Regulatory mechanisms governing the oocyte-specific synthesis of the karyoskeletal protein NO145. *J. Cell. Sci.*, **120**, 1412–1422.
34. Brenner, S., Pepper, D., Berns, M.W., Tan, E. and Brinkley, B.R. (1981) Kinetochore structure, duplication, and distribution in mammalian cells: analysis by human autoantibodies from scleroderma patients. *J. Cell Biol.*, **91**, 95–102.
35. Sharp, P.A. and Burge, C.B. (1997) Classification of introns: U2-type or U12-type. *Cell*, **91**, 875–879.
36. Turunen, J.J., Niemela, E.H., Verma, B. and Frilander, M.J. (2013) The significant other: splicing by the minor spliceosome. *Wiley Interdiscip. Rev. RNA*, **4**, 61–76.
37. Patel, A.A., McCarthy, M. and Steitz, J.A. (2002) The splicing of U12-type introns can be a rate-limiting step in gene expression. *EMBO J.*, **21**, 3804–3815.
38. Bao, J., Yuan, S., Maestas, A., Bhetwal, B.P., Schuster, A. and Yan, W. (2013) Stk31 is dispensable for embryonic development and spermatogenesis in mice. *Mol. Reprod. Dev.*, **80**, 786.
39. Zhou, J., Leu, N.A., Eckardt, S., McLaughlin, K.J. and Wang, P.J. (2014) STK31/TDRD8, a germ cell-specific factor, is dispensable for reproduction in mice. *PLoS One*, **9**, e89471.
40. Carroll, J. and Marangos, P. (2013) The DNA damage response in mammalian oocytes. *Front. Genet.*, **4**, 117.
41. Bolcun-Filas, E., Rinaldi, V.D., White, M.E. and Schimenti, J.C. (2014) Reversal of female infertility by Chk2 ablation reveals the oocyte DNA damage checkpoint pathway. *Science*, **343**, 533–536.
42. Suh, E.K., Yang, A., Kettenbach, A., Bamberger, C., Michaelis, A.H., Zhu, Z., Elvin, J.A., Bronson, R.T., Crum, C.P. and McKeon, F. (2006) P63 protects the female germ line during meiotic arrest. *Nature*, **444**, 624–628.
43. Kerr, J.B., Hutt, K.J., Michalak, E.M., Cook, M., Vandenberg, C.J., Liew, S.H., Bouillet, P., Mills, A., Scott, C.L., Findlay, J.K. *et al.* (2012) DNA damage-induced primordial follicle oocyte apoptosis and loss of fertility require TAp63-mediated induction of puma and noxa. *Mol. Cell*, **48**, 343–352.
44. Yu, J., Hecht, N.B. and Schultz, R.M. (2001) Expression of MSY2 in mouse oocytes and preimplantation embryos. *Biol. Reprod.*, **65**, 1260–1270.
45. Bisig, C.G., Guiraldelli, M.F., Kouznetsova, A., Scherthan, H., Hoog, C., Dawson, D.S. and Pezza, R.J. (2012) Synaptonemal complex components persist at centromeres and are required for homologous centromere pairing in mouse spermatocytes. *PLoS Genet.*, **8**, e1002701.
46. Qiao, H., Chen, J.K., Reynolds, A., Hoog, C., Paddy, M. and Hunter, N. (2012) Interplay between synaptonemal complex, homologous recombination, and centromeres during mammalian meiosis. *PLoS Genet.*, **8**, e1002790.
47. Cocquet, J., Ellis, P.J., Yamauchi, Y., Mahadevaiah, S.K., Affara, N.A., Ward, M.A. and Burgoyne, P.S. (2009) The multicopy gene sly represses the sex chromosomes in the male mouse germline after meiosis. *PLoS Biol.*, **7**, e1000244.
48. Cocquet, J., Ellis, P.J., Yamauchi, Y., Riel, J.M., Karacs, T.P., Rattigan, A., Ojarikre, O.A., Affara, N.A., Ward, M.A. and Burgoyne, P.S. (2010) Deficiency in the multicopy Sycp3-like X-linked genes slx and Slxl1 causes major defects in spermatid differentiation. *Mol. Biol. Cell*, **21**, 3497–3505.
49. Cocquet, J., Ellis, P.J., Mahadevaiah, S.K., Affara, N.A., Vaiman, D. and Burgoyne, P.S. (2012) A genetic basis for a postmeiotic X versus Y chromosome intragenomic conflict in the mouse. *PLoS Genet.*, **8**, e1002900.
50. Soh, Y.Q., Alfoldi, J., Pyntikova, T., Brown, L.G., Graves, T., Minx, P.J., Fulton, R.S., Kremitzki, C., Koutseva, N., Mueller, J.L. *et al.* (2014) Sequencing the mouse Y chromosome reveals convergent gene acquisition and amplification on both sex chromosomes. *Cell*, **159**, 800–813.
51. Eggan, K., Akutsu, H., Loring, J., Jackson-Grusby, L., Klemm, M., Rideout, W.M. III, Yanagimachi, R. and Jaenisch, R. (2001) Hybrid vigor, fetal overgrowth, and viability of mice derived by nuclear cloning and tetraploid embryo complementation. *Proc. Natl. Acad. Sci. U. S. A.*, **98**, 6209–6214.
52. Peters, A.H., Plug, A.W., van Vugt, M.J. and de Boer, P. (1997) A drying-down technique for the spreading of mammalian meiocytes from the male and female germline. *Chromosome Res.*, **5**, 66–68.
53. Wang, P.J. and Page, D.C. (2002) Functional substitution for TAFII250 by a retroposed homolog that is expressed in human spermatogenesis. *Hum. Mol. Genet.*, **11**, 2341–2346.
54. Myers, M., Britt, K.L., Wreford, N.G., Ebling, F.J. and Kerr, J.B. (2004) Methods for quantifying follicular numbers within the mouse ovary. *Reproduction*, **127**, 569–580.